Structural Engineering and Mechanics, Vol. 21, No. 3 (2005) 333-350
DOI: http://dx.doi.org/10.12989/sem.2005.21.3.333

Seismic shear strengthening of R/C beams and columns with expanded steel meshes

Reza Morshed†

Department of Civil Engineering, Yazd University, Yazd, P.O. Box 89195-741, Iran

Mohammad Taghi Kazemi‡

Department of Civil Engineering, Sharif University of Technology, Tehran, P.O. Box 11365-9313, Iran

(Received November 30, 2004, Accepted July 5, 2005)

Abstract. This paper presents results of an experimental study to evaluate a new retrofit technique for strengthening shear deficient short concrete beams and columns. In this technique a mortar jacket reinforced with expanded steel meshes is used for retrofitting. Twelve short reinforced concrete specimens, including eight retrofitted ones, were tested. Six specimens were tested under a constant compressive axial force of 15% of column axial load capacity based on original concrete gross section, A_g, and the concrete compressive strength, f_c'. Main variables were the spacing of ties in original specimens and the volume fraction of expanded metal in jackets. Original specimens failed before reaching their nominal calculated flexural strength, M_n, and had very poor ductility. Strengthened specimens reached their nominal flexural strength and had a ductility capacity factor of up to 8 for the beams and up to 5.5 for the columns. Based on the test results, it can be concluded that expanded steel meshes can be used effectively to strengthen shear deficient concrete members.

Key words: expanded steel mesh; concrete; short column; ductility; shear strength; retrofit; strengthening.

1. Introduction

A large number of existing reinforced concrete structures, which were designed in accordance with old design provisions, could be considered as having poor performance during earthquakes. In some instances, non-ductile short beams and columns with poor seismic detailing are the main cause for structural brittleness. Due to short dowels and little transverse reinforcement, risk of brittle shear failure in such members is very high and premature shear failure decreases ductility capacity of the structures. In order to maintain high ductility capacity in bridge columns, the plastic hinges must form at the ends of columns. It is very important to develop efficient techniques to retrofit shear critical columns and increase their ductility capacity. Wrapping concrete columns with a proper strengthening material can be an effective solution. Reinforced concrete, welded wire fabric and mortar, steel plates, steel straps and fiber reinforced polymer, FRP, composites are common

† Assistant Professor, Corresponding author, E-mail: morshed@yazduni.ac.ir
‡ Associate Professor, E-mail: kazemi@sharif.edu

retrofit techniques (Wipf *et al.* 1997).

Bett *et al.* (1988) studied effectiveness of two concrete jacketing techniques in enhancing the lateral load response of reinforced concrete shear deficient short columns. Based on the results, columns strengthened by jacketing were much stiffer and stronger than the original columns. Priestley *et al.* (1994a, 1994b) investigated a full-height steel jacketing method for retrofitting short shear deficient columns. They used elliptical steel jacket for strengthening rectangular columns to confine the concrete core more effectively although it could considerably increase the cross sectional area and the flexural stiffness of columns. They tested 14 large-scale columns subjected to cyclic shear in double curvature under constant axial load. They found that the brittle shear failure was prevented by steel jacketing retrofit and good ductility capacities were achieved. Aboutaha *et al.* (1996) used rectangular full-height steel jackets for seismic retrofitting of R/C shear columns. Based on the test results, the mode of failure was changed to ductile flexural failure.

The earliest reference located on composite retrofitting of concrete columns was published in Japan by Katsumata *et al.* (1988). They studied the effectiveness of directly winding continuous carbon fiber strands onto the surface of shear deficient rectangular columns and found that the mode of failure was changed from shear to a ductile flexural response. Saadatmanesh *et al.* (1997) investigated seismic strengthening of concrete columns using FRP composite straps. Based on their test results, concrete columns externally wrapped with FRP composite straps in the potential plastic hinge region showed a significance improvement in the both strength and displacement ductility. Xiao *et al.* (1999) investigated seismic shear strengthening of circular concrete columns using full-height prefabricated composite jackets. They concluded that composite jackets could improve ductility and shear strength with minor increase in flexural strength and stiffness of test columns. Sheikh and Yau (2002) investigated the behavior of FRP retrofitted circular columns under simulated earthquake loads. Based on the test results, the FRP wraps effectively confine the entire column section and significantly improve ductility, energy dissipation capacity and strength of columns.

Takiguchi and Abdullah (2001, 2003) performed an experimental research program on the use of ferrocement jackets reinforced with wire meshes for strengthening square reinforced concrete columns with inadequate shear strength. Based on the test results, both circular and square ferrocement jacket could enhance the shear strength and ductility of small-scale square column specimens.

In this research, a thin mortar jacket reinforced with expanded steel mesh (a kind of ferrocement) was used for retrofitting short shear deficient concrete members. New proposed technique can be very cost effective, especially in developing countries. The technique is durable and does not need any special fire or corrosion protection.

Expanded steel meshes are formed by slitting steel sheets and expanding them in a direction perpendicular to the slits. They have a diamond-shaped mesh pattern (Fig. 1). Rolling could flatten these sheets and enhances their performance as reinforcement in concrete or mortar (Khaloo and Morshed 2000). This reinforced concrete or mortar is stronger and relatively stiffer in the long diagonal direction of diamonds and has lower strength and stiffness in the perpendicular direction (ACI 549.1R-93). By wrapping the concrete member with layers of expanded metal and mortar so that the short diagonal direction is in the longitudinal direction of member, the effect of jacket on flexural strength of the member will be minimized. This is relatively similar to the mechanism of FRP composite straps. The rolls of expanded steel meshes are available in different sizes that can be wind on actual large columns in several layers. Stronger meshes are in the shape of steel sheets that may be formed in U, L, or any other suitable, shapes. Two or more of such formed sheets, with lap splices, could be used to jacket large columns.

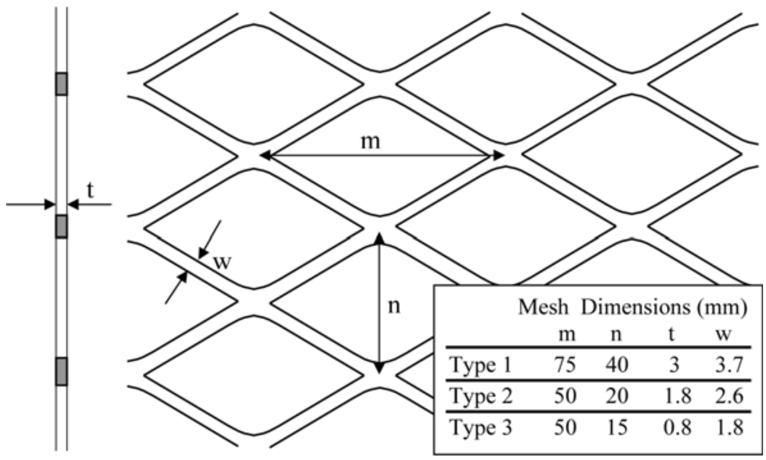

Mesh Dimensions (mm)	m	n	t	w
Type 1	75	40	3	3.7
Type 2	50	20	1.8	2.6
Type 3	50	15	0.8	1.8

Fig. 1 Details of flattened expanded steel meshes

2. Experimental program

A total of twelve shear-critical short concrete columns were built and tested in two stages. The first stage specimens were tested without axial force (beam specimens) while the second stage specimens were tested under a constant compressive axial load (column specimens). The main goal was to test short columns but beams were easy to test to assure of the effectiveness of this new technique in shear retrofitting. A twin shape was selected for the specimens (Fig. 2). Each twin specimen consisted of a thicker and stronger middle part and two cantilever parts at the sides. The middle part was fixed to the testing machine frame and each cantilever part was tested separately. Totally, eight retrofitted and four original cantilever members were tested. Beside these tests, six tensile tests were performed to determine expanded steel meshes properties, three on steel specimens and three on reinforced mortar specimens.

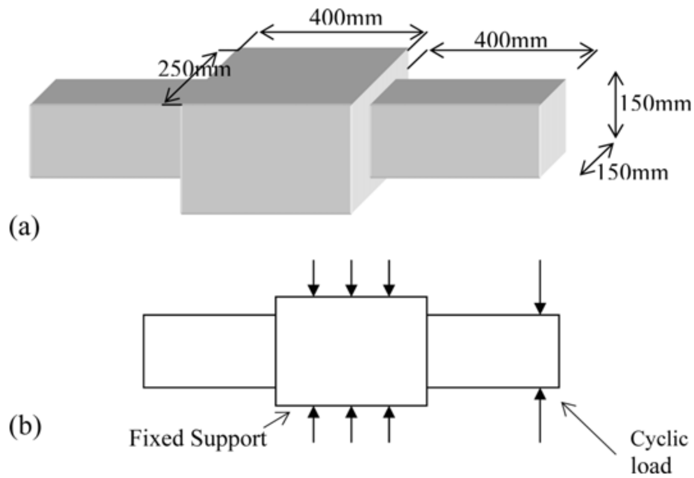

Fig. 2 (a) Dimensions of original twin specimens and (b) Schematic test setup

3. Expanded steel meshes

Three types of expanded steel meshes, which differ in thickness and mesh dimensions, were used in tests (Fig. 1). Although the expanded metal sheets were formed from mild steel meshes but tensile test of steel specimens, cut from the expanded mesh, did not show any indication of yield plateau. They had an average ultimate strength of 470 MPa and nominal yield strength of 400 MPa. Plastic deformations developed in manufacturing process of expanded metal could be the reason. Tensile test of expanded steel mesh embedded in mortar, as recommended by ACI 549.1R-93, also was performed. Three tensile reinforced mortar specimens were designed and built (Fig. 3). They were reinforced with type 1 expanded mesh and tested under pure tension. The middle half of the free portion of the test specimens was instrumented to record elongations (Fig. 3).

The volume fraction of expanded mesh for all of the specimens was 0.022. In two specimens the long diagonal direction of expanded mesh was in the direction of loading (specimens T1 & T2) and in one specimen it was perpendicular to the loading direction (specimen T3). These specimens were built with the same mortar as used in retrofitting concrete column specimens explained later. Fig. 4 shows specimen T1 at the end of tensile test. Transverse cracks are distributed in the specimen's height. Fig. 5 shows experimental load-displacement result for tensile mortar specimens. Displacement ductility capacity factors, defined in Fig. 6, equal to 5 for specimen T1 and 3.5 for specimen T2

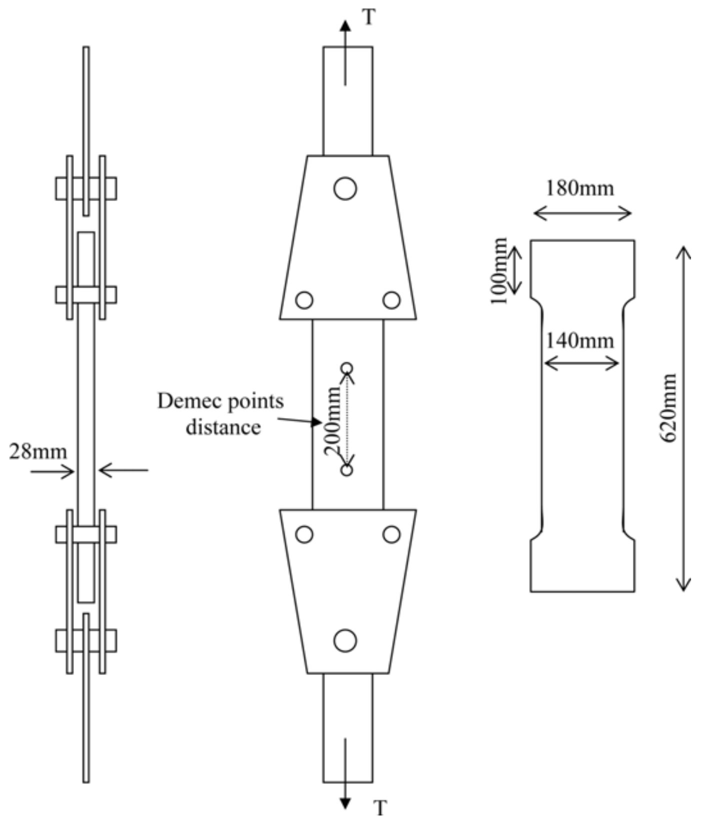

Fig. 3 Details of reinforced mortar tensile specimens

were observed in the long diagonal direction that shows ductile behavior of mortar specimens in this direction (Fig. 5). On the contrary, reinforced mortar specimen in the short diagonal direction of expanded mesh showed a brittle failure and less strength (Fig. 5).

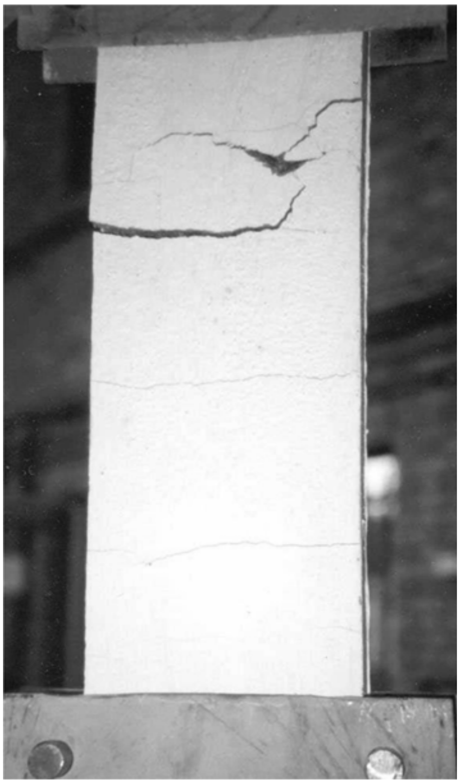

Fig. 4 Reinforced mortar specimen T1 at the end of tensile test

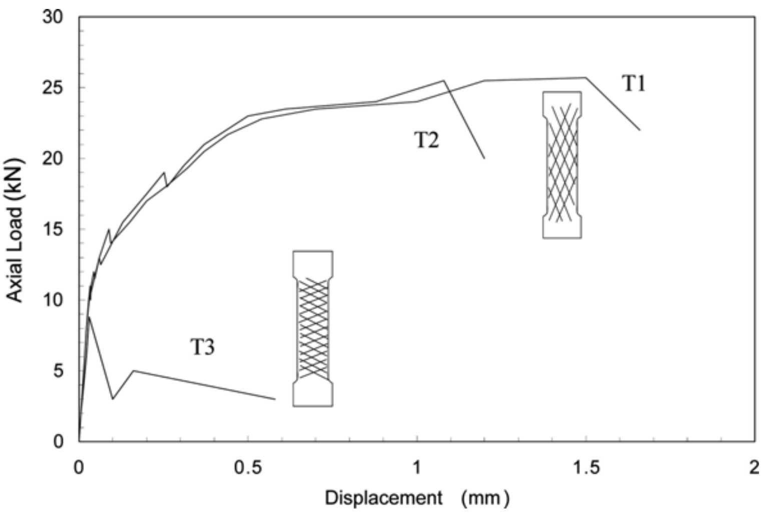

Fig. 5 Load-displacement curves of tensile reinforced mortar specimens

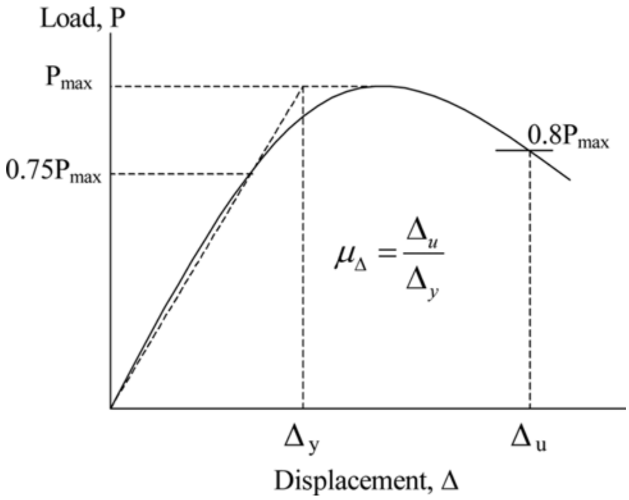

Fig. 6 Definition of displacement ductility capacity factor, μ_Δ

Nominal tensile strength of expanded mesh reinforced mortar can be estimated using the following equation (ACI 549.1R-93):

$$T_n = A_{se} f_y \tag{1}$$

where f_y is the steel yield strength and A_{se} is the effective area of reinforcement and can be defined as follows:

$$A_{se} = \eta \, V_f A_c \tag{2}$$

where:

η = global efficiency factor of mesh reinforcement, 0.65 in the long diagonal direction of expanded mesh and 0.2 in the short diagonal direction

V_f = volume fraction of mesh reinforcement

A_c = gross cross sectional area of mortar section

Tensile strength of specimens was 23 kN in the long diagonal direction of mesh reinforcement (mean of two tests) and 8 kN in the short diagonal direction. These results are equivalent to global efficiency factors of 0.67 and 0.23, respectively, which are in a good agreement with the suggested values of ACI-549.1R-93.

4. Beam specimens

At the first stage, six concrete beam specimens (three twins) were built. The specimens had square sections with 150 millimeters sides and were reinforced as shown in Fig. 7. Variables included tie spacing and concrete compressive strength (Table 1).

Concrete batches were mixed with water to cement ratios of 0.5 and 0.6. Type I Portland cement, natural sand and crushed limestone with maximum size of 19 mm were used. The slump of fresh concrete was about 50 millimeters. Test specimens and their respective concrete cylindrical samples were cured in a moist room until the test time at a temperature of about 23°C. Compressive strength

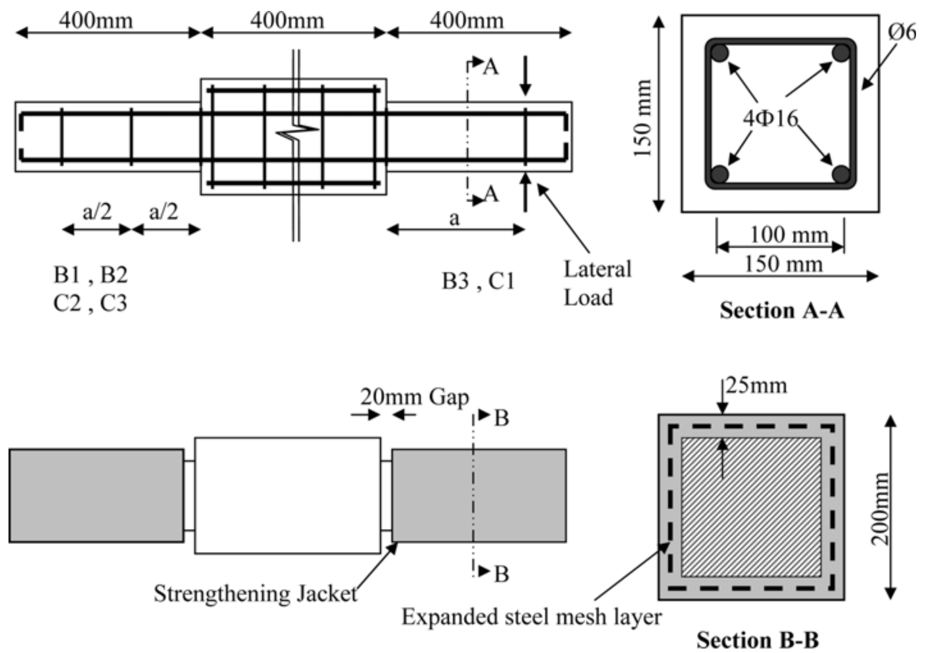

Fig. 7 Details of original and retrofitted specimens, a = 300 & 260 mm for beams and columns, respectively

Table 1 Details of original twin specimens

Specimen No.	Main rebars	Transverse reinforcement	f_c'
Beam specimens			
B1	4Φ16, f_y = 660 MPa	Φ6@150 mm, f_y = 300 MPa	32 MPa
B2	4Φ16, f_y = 660 MPa	Φ6@150 mm, f_y = 300 MPa	25 MPa
B3	4Φ16, f_y = 660 MPa	Φ6@300 mm, f_y = 300 MPa	25 MPa
Column specimens			
Specimen No.	Main rebars	Transverse reinforcement	f_c'
C1	4Φ16, f_y = 500 MPa	Φ6@260 mm, f_y = 300 MPa	35 MPa
C2	4Φ16, f_y = 500 MPa	Φ6@130 mm, f_y = 300 MPa	35 MPa
C3	4Φ16, f_y = 500 MPa	Φ6@130 mm, f_y = 300 MPa	35 MPa

of concrete cylindrical samples, f_c', at the test time were 25 and 32 MPa (Table 1).

Longitudinal reinforcement in all specimens consisted of four Φ16 deformed steel bars with a yield strength of 660 MPa and a center-to-center spacing of 100 millimeters. Transverse reinforcements were ϕ6 mm steel ties with a yield strength of 300 MPa with variable spacing (Table 1).

Two specimens (B1 and B3) were tested without retrofitting and four specimens were tested after retrofitting with 25 millimeters thick mortar jackets reinforced with expanded steel meshes (Fig. 7). There was a 20 millimeters gap between strengthening jacket and the support, the point of maximum flexure, to minimize the increasing of flexural capacity (Fig. 7). The variables were type and volume fraction of expanded meshes and compressive strength of mortar. Shear span was two times the thickness of original specimens. Details of beam specimens are presented at Tables 1 and 2 and are shown in Figs. 2, 7, and 8. The surface of specimen B1-SF was lightly roughened before jacketing but other specimens were retrofitted without any surface treatment.

A shrinkage compensated mortar was used for jacketing with water to cement ratios from 0.4 to 0.5. Natural fine sand passing No.8 sieve and type I Portland cement with equal ratios were used. Expansive grouting admixture at a ratio of about 1 percent of cement weight was added to reduce shrinkage cracking. The compressive strengths of 50 mm mortar cube samples were measured from 22 to 45 MPa (Table 2). Two types of flattened expanded steel meshes were used for jacket reinforcement, type 1 with coarse mesh (specimens B2-SC and B3-SC) and type 2 with fine mesh (specimens B1-SF and B2-SF). Surface unit masses of these expanded steel meshes were 4.8 kg/m^2 and 3.9 kg/m^2 respectively.

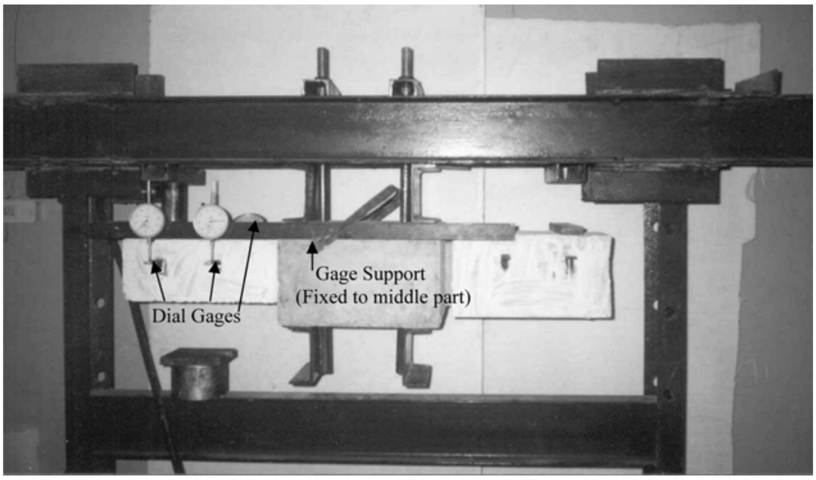

Fig. 8 Test setup for beam specimens

Table 2 Jacketing details of retrofitted specimens

Specimen No.	Jacket reinforcement	Mortar strength
	Beam specimens	
B1-SF	Exp. Mesh, Type 2, $V_f^* = 0.02$	40 MPa
B2-SC	Exp. Mesh, Type 1, $V_f = 0.024$	22 MPa
B2-SF	Exp. Mesh, Type 2, $V_f = 0.02$	45 MPa
B3-SC	Exp. Mesh, Type 1, $V_f = 0.024$	28 MPa
	Column specimens	
Specimen No.	Jacket reinforcement	Mortar strength
C1-SC	One Layer Exp. Mesh, Type 1, $V_f = 0.024$	30 MPa
C2-SF	Two Layers Exp. Mesh, Type 3, $V_f = 0.016$	30 MPa
C3-SF	One Layer Exp. Mesh, Type 3, $V_f = 0.008$	30 MPa
C3-ST	Tie Φ8@90 mm, $V_f = 0.024$	30 MPa

*Volume fraction of jacket reinforcement

4.1 Beam testing procedure and results

Test setup for beam specimens is shown in Figs. 2 and 8. After fixing the specimen to the load frame, cyclic lateral load was applied using a manual hydraulic jack. Due to the limitations of test setup, cyclic lateral displacement was limited to 20 mm. For specimens B2-SC and B2-SF, the lateral load was continued monotonically to the failure of the specimens. Displacements were

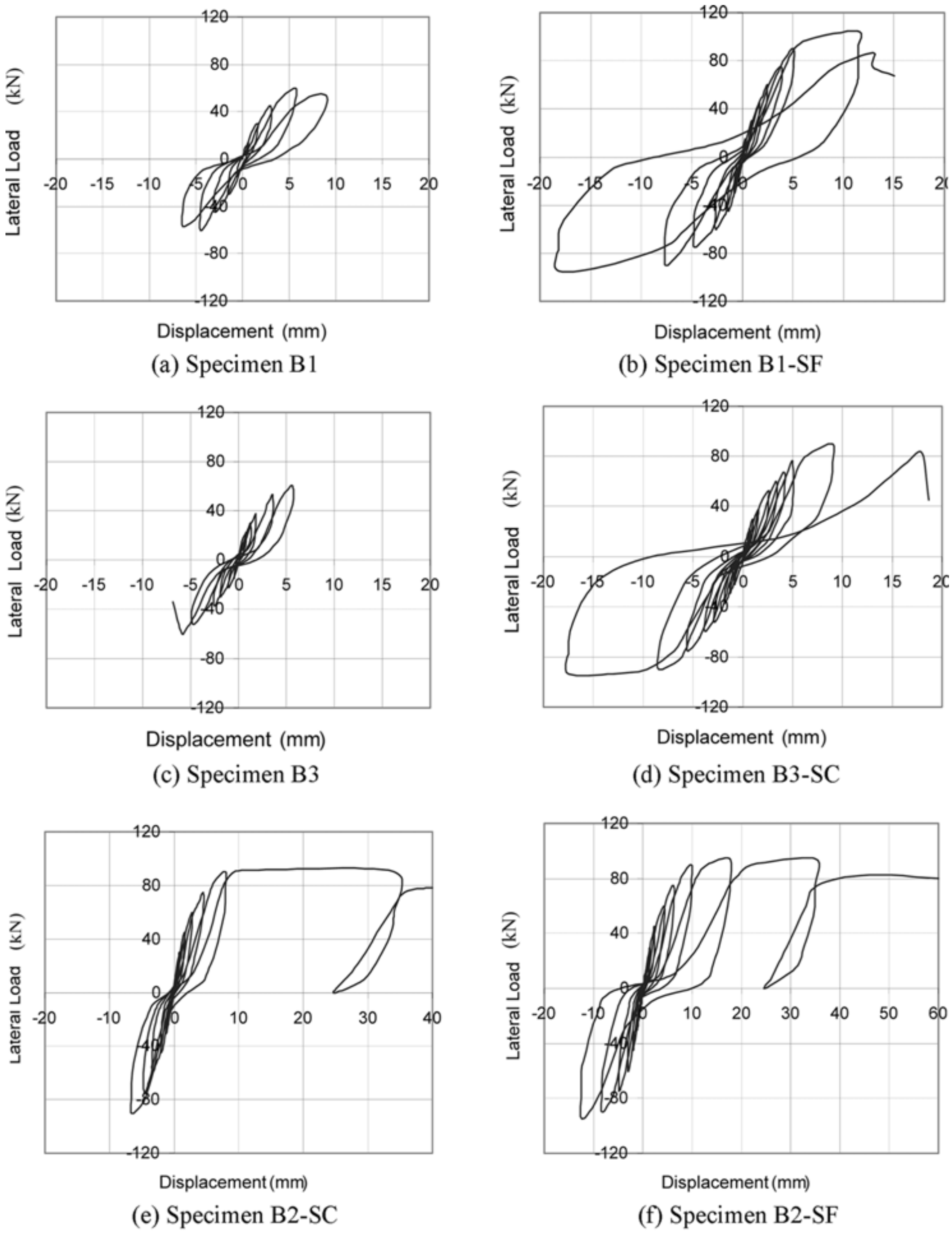

Fig. 9 Experimental cyclic lateral load-displacement curves for beams

measured using mechanical dial gauges with 0.01 millimeters accuracy (Fig. 8). The dial gauges were attached to the stronger middle part of specimens to eliminate reading errors due to frame deformations. During testing, crack patterns and observed damages were recorded with photographs and sketches.

Hysteresis curves of lateral load versus lateral displacement at the loading point are shown in Fig. 9. Pinching observed in the hysteretic behavior is because of cracking and slip between jacket and beam. Specimen B1-SF that had roughened surfaces before jacketing showed less pinching and more strength but its ductility capacity was lower. Surface roughening reduced the slip between specimen and jacket. The cyclic slip between original specimen surface and the strengthening jacket can dissipate a considerable amount of energy and improves the ductility capacity.

In Fig. 10, envelopes of cyclic experimental results are compared. The displacement ductility capacity factor is defined as the ratio of the displacement at a point corresponding to 80% of the maximum lateral load on the descending branch of load-displacement envelope to the yield displacement (Fig. 6). Table 3 gives the displacement ductility capacity factor and limit lateral displacements for the specimens.

Both of the original specimens, B1 and B3, failed in shear before reaching their calculated nominal flexural strength and had a brittle failure with a poor ductility capacity. All of the retrofitted specimens had enough shear strength to reach the nominal flexural capacity, $M_n \approx 27$ kN-m, calculated according to ACI 318 code (2002). They had reasonable displacement ductility capacity factors from 3.2 to 8. Observed ultimate lateral displacements ranged from 6 to 20 percent of 300 mm shear span. These drift ratios are very noticeable for short columns. It must be noted that the displacement ductility capacity factor of 8 and the drift ratio equal to 0.2 were not obtained in fully reversed cyclic loading, as pointed out before, and could be less in such loading.

Crack patterns for strengthened and original specimens were different. In original specimens large dominant diagonal shear cracks with a large opening were observed. In retrofitted specimens, fine distributed cracks were observed in jacket at relatively large displacements (Fig. 11). These shear cracks were not observed at small deflections even after reaching the ultimate flexural capacity of

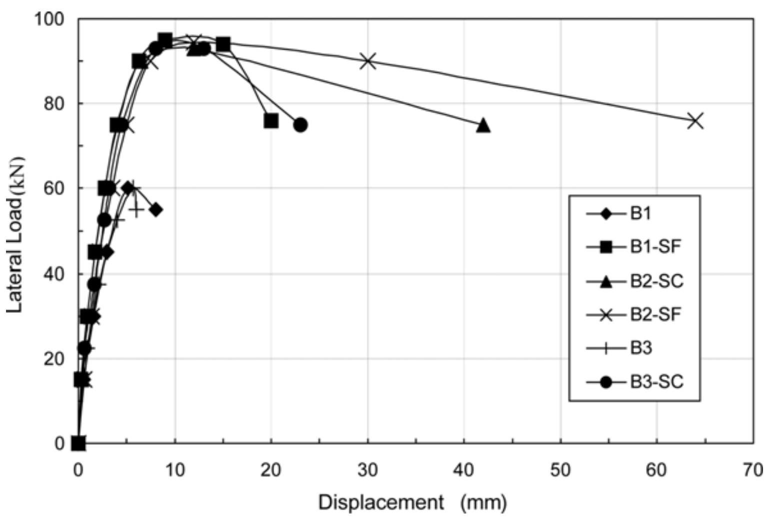

Fig. 10 Envelopes of hysteresis curves for beams

Table 3 Test results for beam specimens

Specimen No.	M_n (kN-m)	$P_{n,\,cal}$ (kN)	P_{test} (kN)	$\Delta_y{}^*$ (mm)	$\Delta_u{}^{**}$ (mm)	μ_Δ
B1	27.4	91.3	60	5	8	1.6
B3	26.9	89.7	60	5	6	1.2
B1-SF	27.4	91.3	97	6	20	3.3
B3-SC	26.9	89.7	93	7	23	3.3
B2-SC	26.9	89.7	93	7	42	6
B2-SF	26.9	89.7	93.5	8	64	8

*Nominal yield displacement (see Fig. 6)
**Nominal displacement capacity (see Fig. 6)

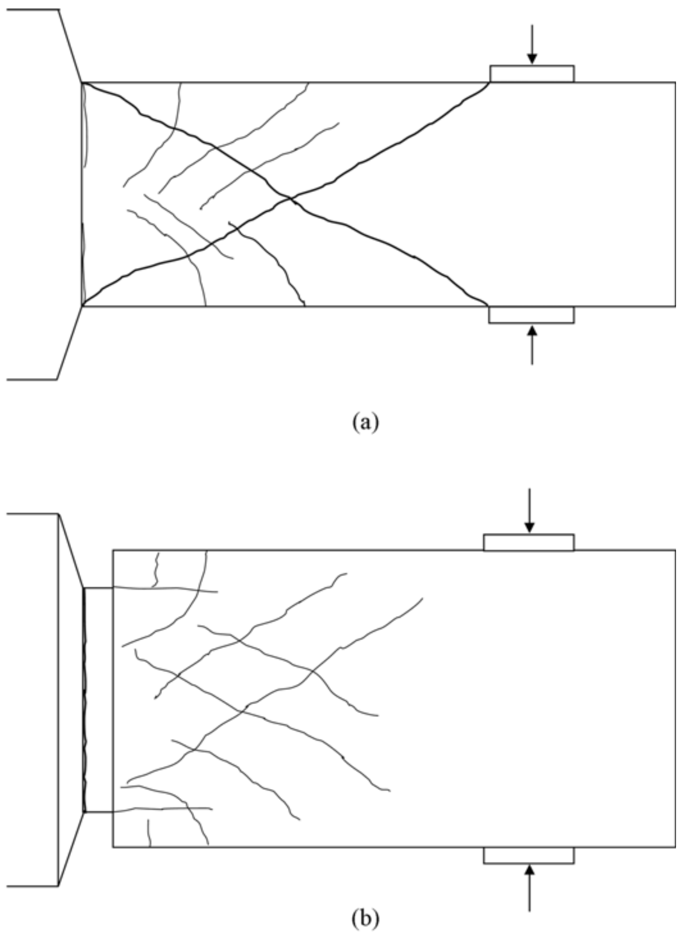

(a)

(b)

Fig. 11 Schematic crack distribution for (a) original and (b) strengthened beams

beams. At the larger deflections, the lateral load capacity of retrofitted beams was reduced and shear cracks in jacket were appeared.

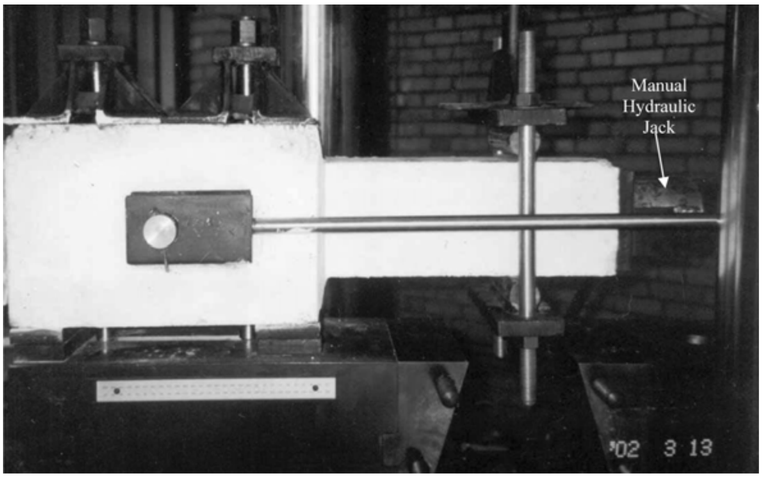

Fig. 12 Test setup for column specimens

5. Column specimens

At this stage, six shear-critical short concrete columns (three twin specimens) were built and tested under constant axial compression of 0.15 $f_c'A_g$ and cyclic lateral load. The same geometry and size of the beam specimens were used for column specimens. With providing a hole in the middle part of the specimens, the application of axial load on columns was made possible (Fig. 12). Tie spacing was the only variable before strengthening (Table 1).

A concrete mix with type I Portland cement, river sand and crushed limestone with maximum size of 19 mm and water to cement ratio equal to 0.5 was used. The slump of the fresh concrete was about 70 millimeters. Test specimens and their respective concrete cylindrical samples were cured in a moist room at a temperature of about 23°C to the test time. Average compressive strength of concrete cylindrical samples, f_c', at the test time was 35 MPa.

Longitudinal reinforcement in all specimens consists of four Φ16 mm deformed steel bars with a yield strength of 500 MPa and a center-to-center spacing of 100 millimeters (Fig. 7). Transverse reinforcement was ϕ6 mm steel ties with a yield strength of 300 MPa.

Four specimens were retrofitted with 25 millimeters thick reinforced mortar jackets. Three jackets were reinforced with expanded steel meshes and one with ties. Similar to the beam specimens, there was a 20 millimeters gap between the jacket and the base. The volume fraction and type of expanded meshes were different and are given in Tables 1, 2, and Fig. 7.

A shrinkage compensated mortar was prepared for jacketing by mixing fine sand and type I Portland cement in equal amounts and expansive grouting admixture at a ratio of 0.01 cement weight. The average compressive strength of 50 mm mortar cube samples was 30 MPa. Two types of flattened expanded steel meshes were used for the jacket reinforcement, type 1 with coarse mesh (specimen C1-SC) and type 3 with fine mesh (specimens C2-SF and C3-SF). Surface unit masses of these expanded steel meshes were 4.8 kg/m^2 and 1.6 kg/m^2 respectively.

During beam specimens testing, some tearing at the edge of expanded meshes near support was observed. This could cause premature failure of jackets, thus for the column specimens the edge of expanded meshes was strengthened by welding a tie or by folding the edge (Fig 13). For

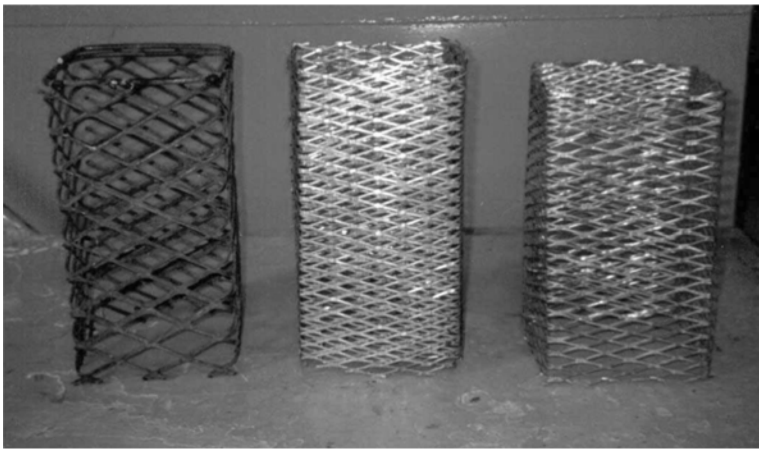

Fig. 13 Prepared expanded steel meshes for retrofitting column specimens

comparison, a column specimen was retrofitted with a mortar jacket reinforced with 8 mm deformed bar ties. Details are given in Table 2.

5.1 Column testing procedure and results

Reversed cyclic lateral displacement was applied by a Dartec 1000 kN universal testing machine with specially designed attachments and setup (Figs. 12 and 14). After fixing the specimen to the testing machine frame, axial load was applied at its predetermined level, 0.15 $f_c'A_g$, by a manual hydraulic jack (Fig. 12). The incremental lateral displacement reversals were applied, with 2 mm increments in the first 5 displacement levels and 5 mm increments in subsequent displacement levels. Two cycles were performed at each displacement level.

Fig. 14 Column specimen under testing by 1000 kN Dartec Universal Testing Machine

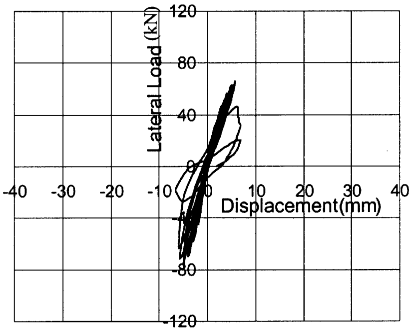

(a) Specimen C1

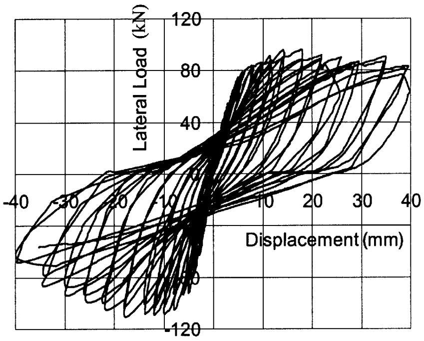

(b) Specimen C1-SC

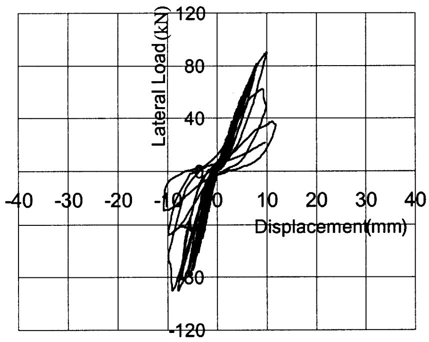

(c) Specimen C2

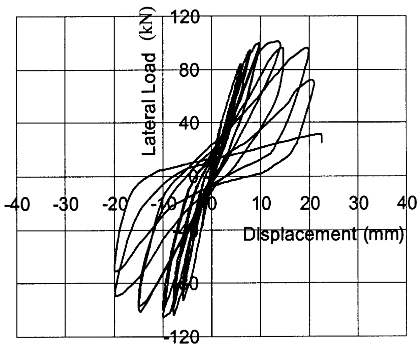

(d) Specimen C2-SF

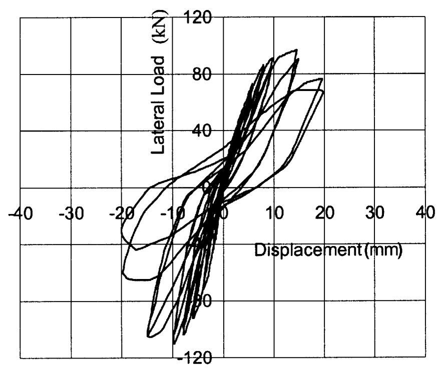

(e) Specimen C3-ST

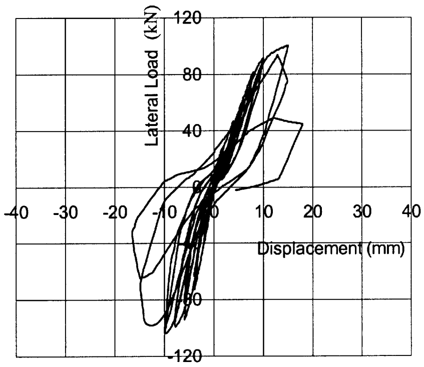

(f) Specimen C3-SF

Fig. 15 Hysteresis curves for column specimens

Hysteresis curves of lateral load versus lateral displacement are shown in Fig. 15. Some pinching is seen in hysteretic behavior that may be due to concrete cracking, bond failure and interface slip. There is also some decrease in lateral stiffness in successive loops. In Fig. 16, envelopes of cyclic experimental results are compared. Displacement ductility capacity factors, defined at Fig. 6, are calculated from these curves. Table 4, summarizes the results for column specimens.

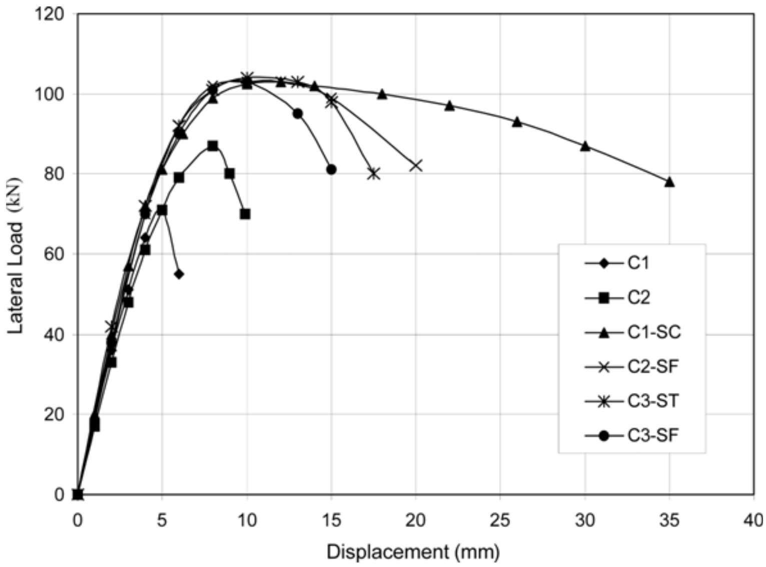

Fig. 16 Envelopes of hysteresis curves for columns

Table 4 Test results for column specimens

Specimen No.	M_n (kN-m)	$P_{n, cal}$ (kN)	P_{test} (kN)	Δ_y^* (mm)	Δ_u^{**} (mm)	μ_Δ
C1	26.6	102	71	4.5	5.5	1.2
C2	26.6	102	88	7	10	1.4
C1-SC	26.6	102	103	6	33	5.5
C2-SF	26.6	102	105	6	20	3.5
C3-ST	26.6	102	105	6	17	2.8
C3-SF	26.6	102	104	6	15	2.5

*Nominal yield displacement (see Fig. 6)
**Nominal displacement capacity (see Fig. 6)

Both of the original specimens (C1 & C2) had a brittle shear failure before reaching their nominal flexural strength capacity and showed poor ductility. All of the retrofitted specimens reached their nominal flexural strength, M_n = 26.6 kN-m, but those retrofitted with lower volume fraction of expanded mesh could not keep their capacity at higher displacement ductility levels (specimens C2-SF & C3-SF). Test results show the interaction between shear strength and ductility. At higher ductility levels the shear strength of specimen decreases and more shear reinforcement is needed to maintain the required shear strength (Priestley *et al*. 1994c, Tumialan *et al*. 2001). Specimen C1-SC showed a ductility factor about twice that of the specimen C3-ST, which was retrofitted with ties with the same steel volume and approximately similar yield strength. In specimen C3-ST, concrete and mortar were completely collapsed at the end of the test (with a lateral displacement of about 20 mm), but the expanded mesh layer could prevent from spalling of core concrete and mortar in specimen C1-SC even at higher ductility levels (Fig. 17). These observations indicate the good performance of expanded meshes in retrofitting concrete columns.

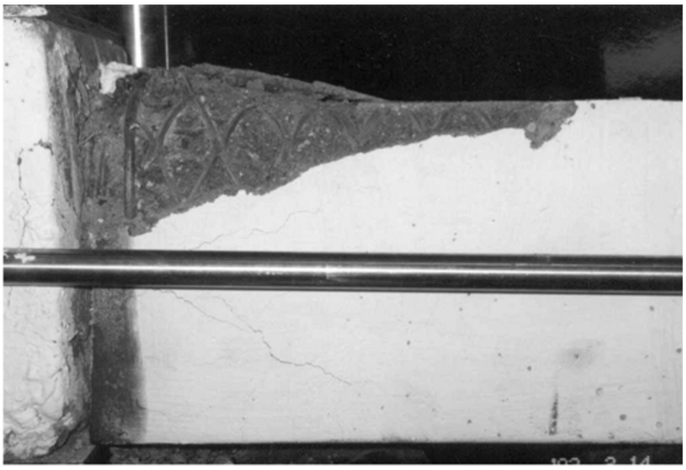

(a)

(b)

Fig. 17 (a) Specimen C1-SC and (b) Specimen C3-ST after completion of tests

It must be noted that the axial loads were limited to the values of 0 and 0.15 $f_c'A_g$. The specimens were, relatively, small scale and size effect could affect the results (Bazant and Kazemi 1991). Columns with larger cross sections are more brittle and shear critical. Large-scale tests and a wider range of axial load are needed to extend and confirm the outcome of this research.

6. Conclusions

Results from the experimental research have been presented in which twelve short concrete specimens were tested under cyclic lateral load. At the first stage, six beam specimens were tested. Four of the specimens were retrofitted with expanded steel meshes before testing. At the second stage, six column specimens were tested under constant axial load equal to 0.15 $f_c'A_g$. Four specimens were retrofitted with expanded steel meshes or ties before testing. The following conclusions can be drawn from this study.

1. Wrapping short shear critical concrete beams and columns, with a layer of mortar reinforced with expanded steel meshes, can significantly increase their shear strength and ductility capacity.
2. The use of expanded meshes can decrease cracking. In comparing the column retrofitted with ties with the specimen that was retrofitted with expanded meshes, the latter, had a more uniformly distributed fine cracking pattern and higher levels of displacement ductility capacity.
3. Relatively small amount of expanded steel meshes (V_f = 0.008) increased shear strength, considerably. However larger steel volume (V_f > 0.02) was needed to attain an acceptable ductility capacity.
4. Roughening the interface between the original beam and the jacket, reduced the pinching, increased the strength, but decreased the ductility capacity.

Acknowledgements

This research work was performed in the Sharif University of Technology, Tehran, Iran. The experimental work was carried out in the Concrete and Structures Laboratories of the Department of Civil Engineering. Assistance from the technical staff is greatly appreciated.

References

Abdullah and Takiguchi, K. (2003), "An investigation into the behavior and strength of reinforced concrete columns strengthened with ferrocement jackets", *Cement & Concrete Composites*, **25**(2), 233-242.

Aboutaha, R.S., Engelhardt, M.D., Jirsa, J.O. and Kreger, M.E. (1996), "Seismic retrofit of R/C columns using steel jackets", ACI Special Publication SP-160, Seismic Rehabilitation of Concrete Structures, 59-72.

ACI Committee 318 (2002), "Building code requirements for structural concrete (ACI 318-02) and commentary (ACI 318R-02)", American Concrete Institute, USA.

ACI Committee 549 (1993), "Guide for the design, construction, and repair of ferrocement (ACI 549.1R-93)," American Concrete Institute, MI, USA.

Bazant, Z.P. and Kazemi, M.T. (1991), "Size effect on diagonal shear failure of beams without stirrups", *ACI Struct. J.*, **88**(3), 268-276.

Bett, B.J., Klinger, R.E. and Jirsa, J.O. (1988), "Lateral load response of strengthened and repaired reinforced concrete columns", *ACI Struct. J.*, **85**, 499-508.

Katsuma, H., Kobatake, Y. and Takeda, T. (1988), "A study on the strengthening with carbon fiber for earthquake resistant capacity of existing reinforced concrete columns", *Proc. of the Ninth World Conf. on Earthquake Engineering*, Tokyo-Kyoto, Japan, **VII**, 517-522.

Khaloo, A.R. and Morshed, R. (2000), "Behavior of concrete slabs reinforced with expanded steel plates", *Proc. of 5th Int. Conf. on Civil Engineering*, Mashhad, Iran, 139-146 (In Persian).

Priestley, M.J.N., Seible, F., Verma, R. and Xiao, Y. (1994a), "Steel jacket retrofitting of reinforced concrete bridge columns for enhanced shear strength – Part 1: Theoretical considerations and test design", *ACI Struct. J.*, **91**(4), 394-405.

Priestley, M.J.N., Seible, F., Verma, R. and Xiao, Y. (1994b), "Steel jacket retrofitting of reinforced concrete bridge columns for enhanced shear strength – Part 2: Test results and comparison with theory", *ACI Struct. J.*, **91**(5), 537-551.

Priestley, M.J.N., Verma, R. and Xiao, Y. (1994c), "Seismic shear strength of reinforced concrete columns", *J. Struct. Eng.*, ASCE, **120**(8), 2310-2329.
Saadatmanesh, H., Ehsani, M.R. and Jin, L. (1997), "Seismic retrofitting of rectangular bridge columns with composite straps", *Earthquake Spectra*, **13**(2), 281-304.
Sheikh, S.A. and Yau, G. (2002), "Seismic behavior of concrete columns confined with steel and fiber-reinforced polymers", *ACI Struct. J.*, **99**(1), 72-80.
Takiguchi, K. and Abdullah (2001), "Shear strengthening of reinforced concrete columns using ferrocement jacket", *ACI Struct. J.*, **98**(5), 696-704.
Tumialan, G., Nakano, K., Fukuyama, H. and Nanni, A. (2001), "Japanese and North American guidelines for strengthening concrete structures with FRP: A comparative review of shear provisions", Non-Metallic Reinforcement for Concrete Structures – FRPRCS-5, Cambridge.
Wipf, T.J., Klaiber, F.W. and Russo, F.M. (1997), "Evaluation of seismic retrofit methods for reinforced concrete bridge columns", Technical Report NCEER-97-0016, NCEER, New York.
Xiao, Y., Wu, H. and Martin, G.R. (1999), "Prefabricated composite jacketing of R/C columns for enhanced shear strength", *J. Struct. Eng.*, ASCE, **125**(3), 255-264.

Notation

A_c : gross cross-sectional area of mortar section
A_g : gross cross-sectional area of original specimens
a : shear span
d : effective depth
f_c' : compressive strength of concrete
f_y : yield strength of steel
M_n : nominal flexural strength calculated according to ACI 318r-02 code
$P_{n,cal}$: calculated nominal lateral load corresponding to M_n
P_{test} : maximum measured test lateral load
T_n : nominal tensile strength of mortar specimens
V_f : volume fraction of mesh reinforcement
Δ_u : postpeak load point displacement corresponding to 80% of peak load
Δ_y : nominal yield load point displacement (defined at Fig. 6)
η : global efficiency factor of mesh reinforcement (ACI 549.1R93)
μ_Δ : displacement ductility capacity factor (defined at Fig. 6)